# Electromagnetic Diffraction of an Obliquely Incident Plane Wave by a Right-Angled Anisotropic Impedance Wedge with a Perfectly Conducting Face

Giuliano Manara, *Senior Member, IEEE*, and Paolo Nepa, *Member, IEEE*

***Abstract*—The diffraction of an arbitrarily polarized electromagnetic plane wave obliquely incident on the edge of a right-angled anisotropic impedance wedge with a perfectly conducting face is analyzed. The impedance tensor on the loaded face has its principal anisotropy axes along directions parallel and perpendicular to the edge, exhibiting arbitrary surface impedance values in these directions. The proposed solution procedure applies both to the exterior and the interior right-angled wedges. The rigorous spectral solution for the field components parallel to the edge is determined through the application of the Sommerfeld–Maliuzhinets technique. A uniform asymptotic solution is provided in the framework of the uniform geometrical theory of diffraction (UTD). The diffracted field is expressed in a simple closed form involving ratios of trigonometric functions and the UTD transition function. Samples of numerical results are presented to demonstrate the effectiveness of the asymptotic expressions proposed and to show that they contain as limit cases all previous three-dimensional (3-D) solutions for the right-angled impedance wedge with a perfectly conducting face.**

***Index Terms*—Electromagnetic diffraction, surface impedance, wedges.**

## I. Introduction

THE increasing interest in anisotropic composite materials for realizing polarization selective surfaces has focused the attention on suitable methods for the analysis of the scattering properties of such surfaces, including the effects introduced by their edges. In most cases, approximate boundary conditions have proved effective to make the scattering problem tractable and to achieve a solution simple to use [1]. For instance, suitable boundary conditions have been derived that couple the tangential field components at the opposite sides of thin composite layers [2], realized by dense planar arrays of complex-shaped scatterers. Also, anisotropic boundary conditions have been applied for analyzing the scattering from planar strip gratings [3] and other periodic surfaces [4], [5] when the period of the structure is much smaller than the free-space wavelength. A validation of the above conditions has been performed in [4] and [5] through comparisons against measurements and moment method data, confirming that these analytical models may represent a viable alternative to more rigorous numerical methods.

In this context, it is worth noting that rigorous three-dimensional (3-D) solutions for electromagnetic scattering from nonperfectly conducting wedges whose faces are modeled by anisotropic impedance boundary conditions (IBC's) are available only for a few specific electrical and geometrical configurations [6]. This observation applies to the simpler case of isotropic IBC's as well [7]. A case of remarkable interest for applications is that of a right-angled impedance wedge. An exact integral solution for this canonical problem has been derived in [8], when the wedge exhibits an isotropic impedance face with the other face perfectly conducting. More recently, the above solution has been extended to analyze the case in which the perfectly conducting face is substituted by an anisotropic impedance face, with a vanishing surface impedance in the direction transverse to the edge [9]. Moreover, a rigorous spectral solution has been derived for a right-angled wedge with both faces characterized by an impedance tensor exhibiting a vanishing surface impedance in the direction parallel to the edge [10]; it remains valid for an arbitrary interior wedge angle. In this framework, we note that from a practical point of view, the presence of a vanishing surface impedance in a principal anisotropy direction may allow us to account for the presence of strip-loaded grounded dielectric slabs with the direction of strips coinciding with that of vanishing surface impedance [11].

A further rigorous spectral solution is derived in this paper when a face of the wedge is characterized by an arbitrary surface impedance tensor with the principal anisotropy axes parallel and perpendicular to the edge and the other face is realized by a perfect electric conductor (PEC) [12]. We note that the solution for the case in which this latter face is constituted by a perfect magnetic conductor (PMC) can be obtained by directly applying duality to the solution valid for the PEC. The analysis is carried out in the case of an arbitrarily polarized plane wave, obliquely incident on the edge of the wedge, both for the exterior and the interior right-angled wedges. The exact integral representation for the total field is determined by resorting to the Sommerfeld–Maliuzhinets method [13]. A pair of decoupled IBC's for each face of the wedge is obtained by expressing the same conditions in terms of suitable linear combinations of the electric and magnetic field components tangential to the loaded face. The problem is then reduced to the solution of a

Manuscript received July 21, 1998; revised December 13, 1999.

The authors are with the Department of Information Engineering, University of Pisa, Pisa, I-56126 Italy.

Publisher Item Identifier S 0018-926X(00)03246-4.

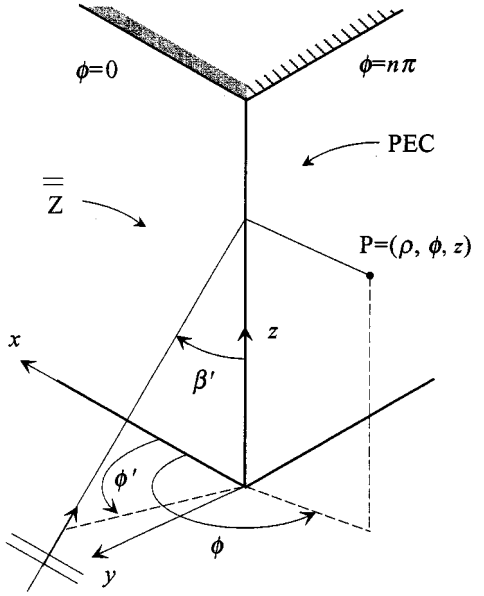


Fig. 1. Geometry for the scattering problem.

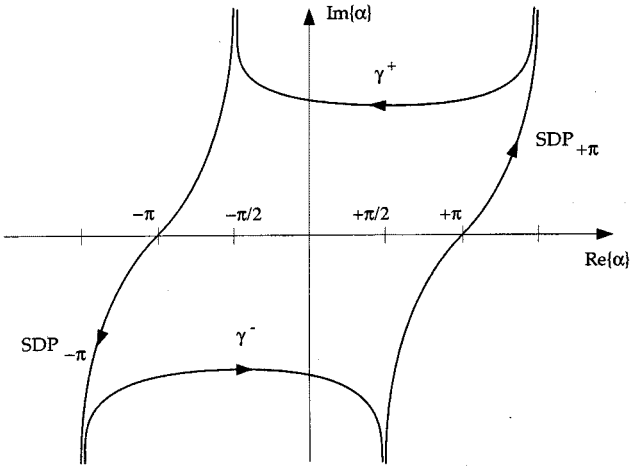


Fig. 2. Integration contours on the complex plane.

set of decoupled functional equations, of the same form as those solved by Maliuzhinets in [13]. The final expressions for the angular spectra of the longitudinal field components can be written in terms of simple trigonometric functions. We note that these spectra involve four constants that are needed to satisfy the edge condition. However, imposing the cancellation of all nonphysical poles enables us to unequivocally determine each constant.

The rigorous spectral representations are then asymptotically evaluated to provide suitable high-frequency expressions for the diffracted field in the format of the uniform geometrical theory of diffraction (UTD). Particular attention is devoted to the phenomenon of surface wave excitation at the edge of the wedge and their propagation along the anisotropic impedance face. As far as the surface wave propagation constants and lit regions are concerned, we note that the results obtained by this analysis remain valid for more general anisotropic wedge configurations, provided that the principal anisotropy directions are parallel and perpendicular to the edge. Finally, it is worth pointing out that the high-frequency expressions proposed yield a uniform behavior of the total field at the shadow boundaries of both the geometrical optics (GO) and the surface wave fields.

The paper has been organized as follows. The formulation of the problem is provided in Section II. The procedure used to reduce the original vector issue to a couple of simpler scalar problems is presented in Section III. Exact integral representations for the longitudinal field components are given in Section IV and suitable uniform asymptotic expressions are provided in Section V. Finally, some numerical results are shown in Section VI to demonstrate that data calculated by these asymptotic expressions exactly coincide with those obtained by all previous solutions for specific configurations contained in the present one as limit cases [8]–[10].

## II. Formulation

The geometry for the scattering problem is shown in Fig. 1. The wedge has its edge overlapped with the $z$-axis of a Cartesian coordinate system $(x, y, z)$; the exterior wedge angle is $n\pi$, $n$ being a real parameter ($n = 3/2$ for the exterior right-angled wedge, $n = 1/2$ for the interior right-angled wedge). The observation point has coordinates $P \equiv (\rho, \phi, z)$ in a cylindrical reference frame with the $z$-axis coincident with that of the above Cartesian system. The face $\phi = 0$ of the wedge lies on the $(x, z)$ plane. The wedge is illuminated by an arbitrarily polarized plane wave impinging from a direction determined by the two angles $\beta'$ and $\phi'$. The angle $\beta'$ is a measure of the incidence direction skewness with respect to the edge of the wedge ($\beta' = \pi/2$ corresponds to normal incidence). An $\exp(j\omega t)$ time dependence is assumed and suppressed. The longitudinal components of the incident field are expressed as

$$E_z^i = e_z e^{-jkz\cos\beta'} e^{jk_t\rho\cos(\phi-\phi')} \tag{1a}$$

$$\zeta H_z^i = h_z e^{-jkz\cos\beta'} e^{jk_t\rho\cos(\phi-\phi')} \tag{1b}$$

where $k$ and $\zeta$ are the wave number and intrinsic impedance of free-space, respectively, and $k_t = k\sin\beta'$ denotes the transverse component of the wave vector. Since the electric properties of the wedge are supposed to be independent of $z$, the scattered field exhibits the same $\exp(-jkz\cos\beta')$ dependence on $z$ as the incident field that will be understood in the following.

Anisotropic IBC's hold on the face $\phi = 0$ of the wedge. In the hypothesis that the principal anisotropy directions are parallel and perpendicular to the edge, the surface impedance is represented by the tensor $\bar{\bar{Z}} = Z_z\hat{z}\hat{z} + Z_x\hat{x}\hat{x}$, with $\mathrm{Re}\{Z_{x,z}\} \geq 0$. Consequently, the IBC's on the face $\phi = 0$ are expressed

$$E_x = Z_x H_z, \quad E_z = -Z_z H_x, \quad \phi = 0. \tag{2}$$

Furthermore, the following boundary conditions must be satisfied at the other face:

$$E_y = 0, \quad E_z = 0, \quad \phi = n\pi. \tag{3}$$

All field components can be written in terms of the longitudinal field components $E_z$ and $\zeta H_z$. The latter components must satisfy the two-dimensional Helmholtz equation and can be expressed in the following spectral form:

$$E_z = \frac{1}{2\pi j}\int_\gamma s_e(\alpha+\phi-n\pi/2)e^{jk_t\rho\cos\alpha}\,d\alpha \quad (4a)$$

$$\zeta H_z = \frac{1}{2\pi j}\int_\gamma s_h(\alpha+\phi-n\pi/2)e^{jk_t\rho\cos\alpha}\,d\alpha \quad (4b)$$

where $\gamma=\gamma^+ + \gamma^-$ is the Sommerfeld integration path depicted in Fig. 2. To satisfy the radiation condition, the spectral functions $s_e(\alpha)$ and $s_h(\alpha)$ must be regular in the strip $|\mathrm{Re}\{\alpha\}| \le n\pi/2$, except for a first-order pole at $\alpha=\phi'-n\pi/2$, accounting for the incident field. Moreover, the edge condition requires that $s_e(\alpha)=\mathcal{O}(1)$ and $s_h(\alpha)=\mathcal{O}(1)$ when $|\mathrm{Im}(\alpha)|\to\infty$. The problem is now reduced to the determination of the spectral functions in (4).

## III. Solution Procedure

By expressing the IBC's in terms of $E_z$ and $\zeta H_z$ we obtain the following differential equations for the anisotropic face:

$$\left\{\frac{1}{\rho}\frac{\partial}{\partial\phi}-jk_t\sin\beta'\frac{\zeta}{Z_z}\right\}E_z - \cos\beta'\frac{\partial}{\partial\rho}(\zeta H_z)=0,\quad \phi=0 \quad (5a)$$

$$\left\{\frac{1}{\rho}\frac{\partial}{\partial\phi}-jk_t\sin\beta'\frac{Z_x}{\zeta}\right\}(\zeta H_z) + \cos\beta'\frac{\partial}{\partial\rho}E_z=0,\quad \phi=0. \quad (5b)$$

Conversely, on the perfectly conducting face ($\phi=n\pi$) the electric and magnetic longitudinal field components must satisfy the standard boundary conditions at the interface with a PEC

$$E_z=0,\quad \phi=n\pi \quad (6a)$$

$$\frac{1}{\rho}\frac{\partial}{\partial\phi}(\zeta H_z)=0,\quad \phi=n\pi. \quad (6b)$$

As apparent, the IBC's in (5) are coupled, i.e., each equation contains both $E_z$ and $\zeta H_z$. However, for the configuration analyzed in this paper, the problem can be scalarized by expressing the IBC's on both wedge faces with respect to the following linear combinations of the field components:

$$\mathcal{E}=\zeta E_z/Z_z+\zeta H_x \quad (7a)$$

$$\zeta\mathcal{H}=Z_x H_z - E_x. \quad (7b)$$

Indeed, by expressing the IBC's at the face $\phi=0$ in terms of $\mathcal{E}$ and $\mathcal{H}$ we obtain

$$\mathcal{E}=0,\quad \zeta\mathcal{H}=0,\quad \phi=0. \quad (8)$$

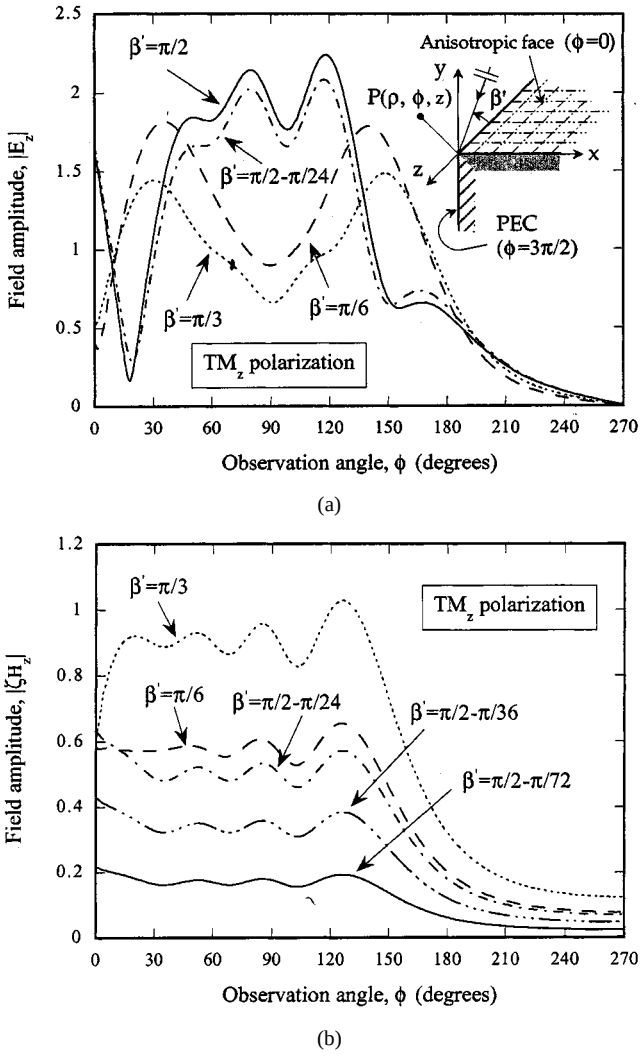


Fig. 3. Amplitude of the (a) copolar and (b) cross-polar longitudinal components of the total field in the presence of a right-angled impedance wedge with the face $\phi=3\pi/2$ perfectly conducting. The wedge is illuminated by a TM$_z$ polarized ($E_z^i=1, \zeta H_z^i=0$) plane wave, impinging from $\phi'=\pi/12$, with different values of the skewness angle $\beta'$. Other geometrical and electrical parameters: $k\rho\sin\beta'=10$, $Z_z/\zeta=-4j$, $Z_x/\zeta=0.25j$.

Furthermore, on the perfectly conducting face ($\phi=n\pi$) both $E_z$ and $H_x$, as well as any linear combination of the two, must satisfy a soft condition. As far as $E_x$ and $H_z$ are concerned, we note that they must meet a hard condition at the same face; of course, the same condition must be fulfilled by any linear combination of the same components. As a consequence of the above observations, the IBC's on the face $\phi=n\pi$ assume the following form:

$$\mathcal{E}=0,\quad \frac{1}{\rho}\frac{\partial}{\partial\phi}(\zeta\mathcal{H})=0,\quad \phi=n\pi. \quad (9)$$

Since both $\mathcal{E}$ and $\zeta\mathcal{H}$ in (7) are solutions of the scalar Helmholtz equation, they can be expressed in terms of Sommerfeld integrals

$$\mathcal{E}=\frac{1}{2\pi j}\int_\gamma t_{\mathcal{E}}(\alpha+\phi-n\pi/2)e^{jk_t\rho\cos\alpha}\,d\alpha \quad (10a)$$

$$\zeta\mathcal{H} = \frac{1}{2\pi j}\int_{\gamma} t_{\mathcal{H}}(\alpha+\phi-n\pi/2)e^{jk_t\rho\cos\alpha}\,d\alpha. \quad (10b)$$

By substituting the previous spectral representations into the IBC's in (8) and (9), a set of decoupled first-order difference equations is obtained [14]

$$t_{\mathcal{E}}(\alpha\mp n\pi/2) - t_{\mathcal{E}}(-\alpha\mp n\pi/2) = 0 \quad (11a)$$
$$t_{\mathcal{H}}(\alpha\mp n\pi/2) \mp t_{\mathcal{H}}(-\alpha\mp n\pi/2) = 0. \quad (11b)$$

They are similar to those obtained by Maliuzhinets for the isotropic impedance wedge, illuminated at normal incidence [13]. Strictly speaking, the Maliuzhinets theorem in [14] requires the inclusion of a forcing term at the second member of (11), consisting of a polynomial in $\cos(\alpha)$. However, we note that for the configuration under analysis, these polynomials must not be introduced since the solution of (11) itself satisfies both the radiation and the edge conditions. Once the expressions for $t_{\mathcal{E}}(\alpha)$ and $t_{\mathcal{H}}(\alpha)$ have been derived, the rigorous solution for the spectra of the longitudinal field components can be obtained by (12), shown at the bottom of the page, where

$$\begin{aligned}\Delta(\alpha) &= (\sin\alpha - \sin\beta'\zeta/Z_z)(\sin\alpha - \sin\beta' Z_x/\zeta)\\ &\quad + \cos^2\alpha\cos^2\beta'\\ &= \sin^2\beta'(\sin\alpha - \sin\vartheta^+)(\sin\alpha - \sin\vartheta^-)\end{aligned} \quad (13)$$

with

$$\sin\vartheta^{\pm} = \frac{1}{2\sin\beta'}\left\{\left(\frac{Z_x}{\zeta}+\frac{\zeta}{Z_z}\right) \pm \left[\left(\frac{Z_x}{\zeta}-\frac{\zeta}{Z_z}\right)^2 + 4\left(\frac{Z_x}{Z_z}-1\right)\cos^2\beta'\right]^{1/2}\right\} \quad (14)$$

and $0 \le \mathrm{Re}(\vartheta^{\pm}) \le \pi/2$. Complete expressions for $t_{\mathcal{E}}(\alpha)$ and $t_{\mathcal{H}}(\alpha)$ will be provided in the next section.

It is worth noting that the definition of suitable potential functions is a crucial point to decouple the anisotropic IBC's on both wedge faces and reduce the original issue to a couple of scalar problems. The potential functions defined in (7) differ from those applied in previous papers [6], [9], and [10]; indeed, their choice strongly depends on the geometrical and electrical configuration under analysis.

## IV. Exact Spectral Solution

By accounting for the radiation and the edge conditions, the solution for the functional equations in (11) can be expressed as [13], [14]

$$t_{\mathcal{E}}(\alpha) = A_{\mathcal{E}}\sigma(\alpha) + C_{\mathcal{E}} + C'_{\mathcal{E}}\sin(\alpha/n) \quad (15a)$$

$$t_{\mathcal{H}}(\alpha) = \frac{\cos\left(\frac{\alpha}{2n}+\frac{\pi}{4}\right)}{\cos\left(\frac{\phi'}{2n}\right)}[A_{\mathcal{H}}\sigma(\alpha) + C_{\mathcal{H}} + C'_{\mathcal{H}}\sin(\alpha/n)] \quad (15b)$$

where

$$\sigma(\alpha) = \frac{1}{n}\frac{\sin\left(\frac{\phi'}{n}\right)}{\sin\left(\frac{\alpha}{n}\right)+\cos\left(\frac{\phi'}{n}\right)} \quad (16)$$

and $C'_{\mathcal{E}} = C'_{\mathcal{H}} = 0$ when $n = 1/2$. The function $\sigma(\alpha)$ introduces a first order pole singularity at $\alpha = \phi' - n\pi/2$, which is needed to recover the incident field; in particular, by imposing that the residues of $s_e(\alpha)$ and $s_h(\alpha)$ coincide with the complex amplitude of the incident field longitudinal components in (1), i.e., $e_z$ and $h_z$, the following values for the constants $A_{\mathcal{E}}$ and $A_{\mathcal{H}}$ are determined:

$$\begin{aligned}A_{\mathcal{E}} = -[&(\sin\phi' - \sin\beta'\zeta/Z_z)e_z\\ &- \cos\phi'\cos\beta' h_z]/\sin\beta'\end{aligned} \quad (17a)$$

$$\begin{aligned}A_{\mathcal{H}} = -[&(\sin\phi' - \sin\beta' Z_x/\zeta)h_z\\ &+ \cos\phi'\cos\beta' e_z]/\sin\beta'.\end{aligned} \quad (17b)$$

The other constants appearing in the solution provide the proper behavior of the spectral functions when $|\mathrm{Im}(\alpha)| \to \infty$; they are determined by imposing the cancellation of specific nonphysical poles introduced by the term $\Delta(\alpha+n\pi/2)$ in (12). Indeed, the term $\Delta(\alpha + n\pi/2)$ introduces pole singularities which are located at

$$\alpha_p^{\pm} = (-1)^N\vartheta^{\pm} - n\pi/2 + N\pi \quad (18)$$

with $N = 0, \pm1, \pm2, \ldots$. The poles in (18) lying in the strip $|\mathrm{Re}\{\alpha\}| \le n\pi/2$ must be cancelled out since they give rise to residue contributions not satisfying the radiation condition. The

$$s_e(\alpha) = \frac{-\sin\beta'\left[t_{\mathcal{E}}(\alpha)\left(\sin\left(\alpha+\frac{n\pi}{2}\right) - \sin\beta'\frac{Z_x}{\zeta}\right) + t_{\mathcal{H}}(\alpha)\cos\left(\alpha+\frac{n\pi}{2}\right)\cos\beta'\right]}{\Delta(\alpha+n\pi/2)} \quad (12a)$$

$$s_h(\alpha) = \frac{-\sin\beta'\left[t_{\mathcal{H}}(\alpha)\left(\sin\left(\alpha+\frac{n\pi}{2}\right) - \sin\beta'\frac{\zeta}{Z_z}\right) - t_{\mathcal{E}}(\alpha)\cos\left(\alpha+\frac{n\pi}{2}\right)\cos\beta'\right]}{\Delta(\alpha+n\pi/2)} \quad (12b)$$

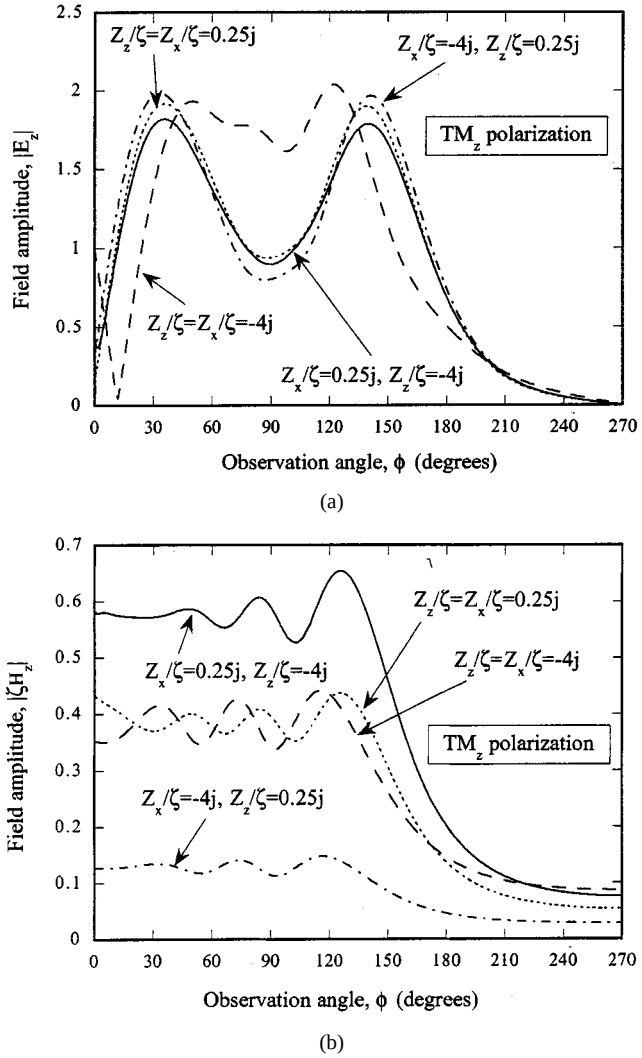


Fig. 4. Amplitude of the (a) copolar and (b) cross-polar longitudinal components of the total field in the presence of a right-angled impedance wedge with the face $\phi = 3\pi/2$ perfectly conducting. The wedge is illuminated by a TM$_z$ polarized ($E_z^i = 1, \zeta H_z^i = 0$) plane wave, impinging from $\beta' = \pi/6$, $\phi' = \pi/12$. Anisotropic cases: $Z_z/\zeta = -4j$, $Z_x/\zeta = 0.25j$ (continuos lines); $Z_z/\zeta = 0.25j$, $Z_x/\zeta = -4j$ (dashed-dotted lines). Isotropic cases: $Z_z/\zeta = Z_x/\zeta = -4j$ (dashed lines); $Z_z/\zeta = Z_x/\zeta = 0.25j$ (dotted lines). The field is evaluated at a normalized distance $k\rho \sin \beta' = 10$ from the edge.

cancellation of these nonphysical poles is obtained by imposing the following conditions:

$$\left[\sin\left(\alpha_p^{\pm} + n\pi/2\right) - \sin\beta' Z_x/\zeta\right] t_{\mathcal{E}}\left(\alpha_p^{\pm}\right) + \cos\beta' \cos\left(\alpha_p^{\pm} + n\pi/2\right) t_{\mathcal{H}}\left(\alpha_p^{\pm}\right) = 0 \tag{19}$$

$$\left[\sin\left(\alpha_p^{\pm} + n\pi/2\right) - \sin\beta' \zeta/Z_z\right] t_{\mathcal{H}}\left(\alpha_p^{\pm}\right) - \cos\beta' \cos\left(\alpha_p^{\pm} + n\pi/2\right) t_{\mathcal{E}}\left(\alpha_p^{\pm}\right) = 0 \tag{20}$$

which guarantee the vanishing of the residues of both $s_e(\alpha)$ and $s_h(\alpha)$ at $\alpha = \alpha_p^{\pm}$. However, it can be shown that once the cancellation of the nonphysical poles of $s_e(\alpha)$ has been imposed, also the elimination of the poles of $s_h(\alpha)$ is automatically obtained, and vice versa. In the right-angled exterior wedge case ($n = 3/2$), four poles arise with residue contributions not satisfying the radiation condition; indeed, these poles lie in the strip $|\mathrm{Re}\{\alpha\}| \le 3\pi/4 : \vartheta^{\pm} - 3\pi/4, -\vartheta^{\pm} + \pi/4$. By applying (19) or (20), a linear equation system is obtained

$$[\sin\vartheta^{\pm} - \sin\beta' Z_x/\zeta] t_{\mathcal{E}}(\vartheta^{\pm} - 3\pi/4) + \cos\beta' \cos\vartheta^{\pm} t_{\mathcal{H}}(\vartheta^{\pm} - 3\pi/4) = 0 \tag{21}$$

$$[\sin\vartheta^{\pm} - \sin\beta' Z_x/\zeta] t_{\mathcal{E}}(-\vartheta^{\pm} + \pi/4) - \cos\beta' \cos\vartheta^{\pm} t_{\mathcal{H}}(-\vartheta^{\pm} + \pi/4) = 0 \tag{22}$$

from which the constants $C_{\mathcal{E}}, C'_{\mathcal{E}}, C_{\mathcal{H}}$ and $C'_{\mathcal{H}}$ can be evaluated. Conversely, in the right-angled interior wedge case ($n = 1/2$), only two poles lie in the strip $|\mathrm{Re}\{\alpha\}| \le \pi/4 : \vartheta^{\pm} - \pi/4$. By imposing the cancellation of these poles a linear equation system is obtained from which the two constants $C_{\mathcal{E}}$ and $C_{\mathcal{H}}$ can be determined

$$[\sin\vartheta^{\pm} - \sin\beta' Z_x/\zeta] t_{\mathcal{E}}(\vartheta^{\pm} - \pi/4) + \cos\beta' \cos\vartheta^{\pm} t_{\mathcal{H}}(\vartheta^{\pm} - \pi/4) = 0. \tag{23}$$

Finally, we observe that the rigorous expressions for the spectra $t_{\mathcal{E}}(\alpha)$ and $t_{\mathcal{H}}(\alpha)$ in (15) and, consequently, those for the longitudinal components $s_e(\alpha)$ and $s_h(\alpha)$ in (12), do not explicitly contain the Maliuzhinets special function [13]. This is in agreement with previous solutions [8]–[10] since for $n = 3/2$ the Maliuzhinets special function reduces to a ratio of simple trigonometric functions.

## V. Asymptotic Analysis

By taking into account (4), (12), and (15), the longitudinal field components $E_z$ and $\zeta H_z$ are expressed in a form suitable for their uniform asymptotic evaluation. In particular, by applying the residue theorem, the original integral representation for the total field along the Sommerfeld integration contour $\gamma$ is reduced to the contribution of: 1) the residues of both GO and surface wave poles, which can be captured in the contour deformation process and 2) two integrals defined along the steepest descent paths SDP$_{\pm\pi}$ through the saddle points at $\pm\pi$ (Fig. 2), providing the edge diffracted field contribution. A uniform asymptotic expression for the field diffracted by the edge, valid also when the poles $\alpha_i$ cross the integration path away from the saddle points, is given by [15]

$$E_z^d = -\frac{e^{-j\pi/4} e^{-jk_t\rho}}{\sqrt{2\pi k_t \rho}} \left( s_e(\pi + \phi - n\pi/2) - s_e(-\pi + \phi - n\pi/2) - \sum_i \mathrm{Res}\{s_e(\alpha), \alpha = \alpha_i\} \times \frac{1 - F(\sqrt{k_t\rho[1 + \cos(\alpha_i - \phi + n\pi/2)]})}{2\cos((\alpha_i - \phi + n\pi/2)/2)} \right) \tag{24a}$$

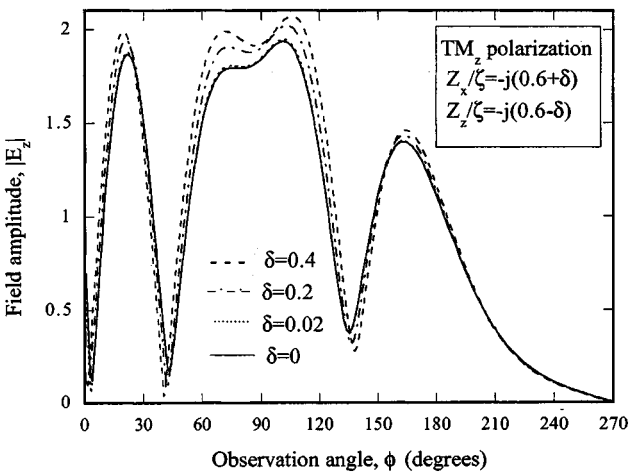


(a)

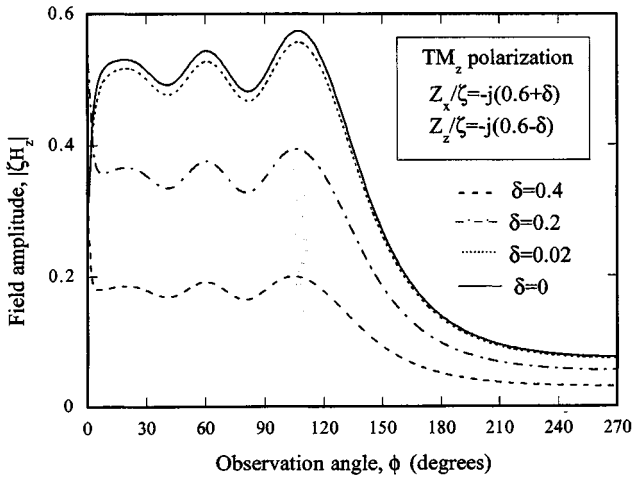


(b)

Fig. 5. Amplitude of the (a) copolar and (b) cross-polar longitudinal components of the total field in the presence of a right-angled impedance wedge with the face $\phi = 3\pi/2$ perfectly conducting. The wedge is illuminated by a TM$_z$ polarized ($E_z^i = 1, \zeta H_z^i = 0$) plane wave, impinging from $\beta' = \pi/4$, $\phi' = \pi/6$. The normalized surface impedances are equal to: $Z_z/\zeta = -j(0.6 - \delta)$, $Z_x/\zeta = -j(0.6 + \delta)$. Dashed lines: $\delta = 0.4$; dashed-dotted lines: $\delta = 0.2$; dotted lines: $\delta = 0.02$; continuous lines: $\delta = 0$ (isotropic impedance face). The field is evaluated at a normalized distance $k\rho \sin\beta' = 10$ from the edge.

$$\zeta H_z^d = -\frac{e^{-j\pi/4}e^{-jk_t\rho}}{\sqrt{2\pi k_t\rho}}\left(s_h(\pi+\phi-n\pi/2) - s_h(-\pi+\phi-n\pi/2) - \sum_i \mathrm{Res}\{s_h(\alpha), \alpha=\alpha_i\} \times \frac{1-F(\sqrt{k_t\rho[1+\cos(\alpha_i-\phi+n\pi/2)]})}{2\cos((\alpha_i-\phi+n\pi/2)/2)}\right) \quad (24b)$$

where $F(\cdot)$ is the UTD transition function [16] generalized to complex arguments as in [15]. The summation appearing in (24) includes all those pole singularities, which result to be the closest to the steepest descent paths SDP$_{\pm\pi}$, when the observation angle varies between $\phi = 0$ and $\phi = n\pi$. It is worth noting that those terms of the summation in (24) accounting for the surface wave poles (complex poles) provide significant contributions to the field when the observation point approaches the impedance face. This verifies even when the corresponding surface wave does not satisfy the excitation condition on the same face. In the latter case, when the observation point moves toward the impedance face, the specific complex pole approaches the SDP$_{-\pi}$ but does not cross the path. However, although always remaining external to the closed contour formed by $\gamma$ and the SDP$_{\pm\pi}$, the vicinity of the pole to the integration path provides a contribution to the diffraction integral which is comparable with the standard UTD approximation [16]. By comparing the results obtained by (24) with reference data provided by a direct numerical integration of the diffraction integral along the SDP$_{\pm\pi}$, a very good agreement is observed [17] even when the observation point is close to the impedance face.

The residues of the pole singularities of $s_e(\alpha)$ and $s_h(\alpha)$ at $\alpha = \phi' - n\pi/2$ and $\alpha = -\phi' + 3n\pi/2$ provide the contribution of the incident field in (1) and that of the field reflected by the perfectly conducting face ($\phi = n\pi$), respectively. In particular, the latter contribution has the following expression:

$$E_z^n = -e_z e^{jk_t\rho\cos(2n\pi-\phi-\phi')}U(\pi+\phi'+\phi-2n\pi) \quad (25a)$$

$$\zeta H_z^n = h_z e^{jk_t\rho\cos(2n\pi-\phi-\phi')}U(\pi+\phi'+\phi-2n\pi) \quad (25b)$$

where $U(\cdot)$ is the Heaviside unit step function.

Moreover, the pole at $\alpha = -\phi' - n\pi/2$ accounts for the field reflected from the anisotropic impedance face ($\phi = 0$). The expression for this residue contribution is

$$E_z^0 = [R_{EE}e_z + R_{EH}h_z]e^{jk_t\rho\cos(\phi+\phi')}U(\pi-\phi'-\phi) \quad (26a)$$

$$\zeta H_z^0 = [R_{HH}h_z + R_{HE}e_z]e^{jk_t\rho\cos(\phi+\phi')}U(\pi-\phi'-\phi) \quad (26b)$$

where

$$R_{EE} = ((\sin\phi' + \sin\beta' Z_x/\zeta)(\sin\phi' - \sin\beta'\zeta/Z_z) - \cos^2\beta'\cos^2\phi')/\Delta(-\phi'), \quad (27)$$

$$R_{HH} = ((\sin\phi' + \sin\beta'\zeta/Z_z)(\sin\phi' - \sin\beta' Z_x/\zeta) - \cos^2\beta'\cos^2\phi')/\Delta(-\phi') \quad (28)$$

and

$$R_{EH} = -R_{HE} = -\cos\beta'\sin(2\phi')/\Delta(-\phi'). \quad (29)$$

Moreover, in the case of the right-angled interior wedge the poles at $\alpha_p = \phi' - 5\pi/4$ and $\alpha_p = \phi' + 3\pi/4$ account for the double reflection term. More precisely, just one of these two poles lies between the two SDP$_{\pm\pi}$, the former when $\phi < \phi'$

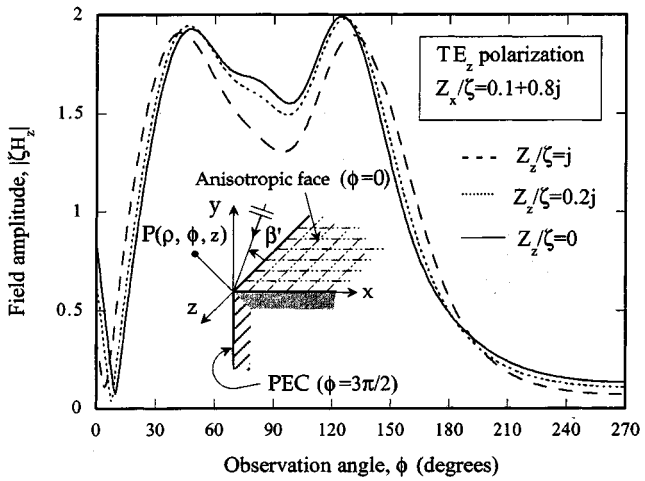


(a)

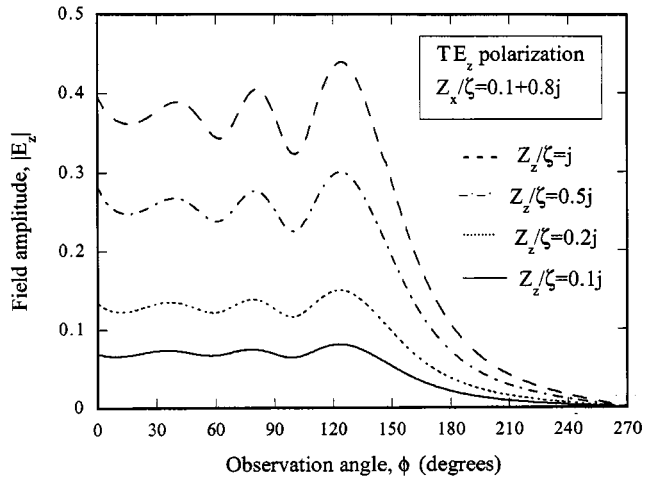


(b)

Fig. 6. Amplitude of the (a) copolar and (b) cross-polar longitudinal components of the total field in the presence of a right-angled impedance wedge with the face $\phi = 3\pi/2$ perfectly conducting. The wedge is illuminated by a TE$_z$ polarized ($E_z^i = 0, \zeta H_z^i = 1$) plane wave, impinging from $\beta' = \pi/4$, $\phi' = \pi/12$. The normalized surface impedance along $x$ is $Z_x/\zeta = 0.1 + 0.8j$. (a) Dashed line: $Z_z/\zeta = j$; dotted line: $Z_z/\zeta = 0.2j$; continuous line: $Z_z/\zeta = 0$. (b) Dashed line: $Z_z/\zeta = j$; dashed-dotted line: $Z_z/\zeta = 0.5j$; dotted line: $Z_z/\zeta = 0.2j$; continuous line: $Z_z/\zeta = 0.1j$. The field is calculated at a normalized distance $k\rho \sin\beta' = 10$ from the edge.

and the latter when $\phi > \phi'$; since their residues coincide, the solution does not show a discontinuity at $\phi = \phi'$. The doubly reflected terms of the longitudinal field components have the following expressions:

$$E_z^{0n} = [-R_{EE}e_z - R_{EH}h_z]e^{-jk_t\rho\cos(\phi-\phi')} \quad (30a)$$

$$\zeta H_z^{0n} = [R_{HH}h_z + R_{HE}e_z]e^{-jk_t\rho\cos(\phi-\phi')}. \quad (30b)$$

Other poles which can be captured in the integration path deformation process are those introduced by the term $\Delta(\alpha+n\pi/2)$ in (12) and external to the strip $|\mathrm{Re}\{\alpha\}| \leq n\pi/2$. In particular, this conditions may be met by the poles at $\alpha_p^{\pm} = \vartheta^{\pm} + 5\pi/4, -\vartheta^{\pm} + 9\pi/4$, for $n = 3/2$, and $\alpha_p^{\pm} = -\vartheta^{\pm} + 3\pi/4$ for $n = 1/2$, respectively. However, by resorting to the functional equations in (11) it can be shown that (21)–(23) also guarantee the cancellation of the above poles for $n = 3/2$ and $n = 1/2$, respectively. This cancellation was expected since the face $\phi = n\pi$ is perfectly conducting and cannot support any surface wave. Finally, for both right-angled configurations the poles at $\alpha_p^{\pm} = -\pi - \vartheta^{\pm} - n\pi/2$ are associated with the two surface waves, which can be excited at the edge and propagate along the impedance face ($\phi = 0$). Their contributions assume the following form:

$$E_z^{\pm} = C_e^{\pm} e^{-jk_t\rho\cos(\phi+\vartheta^{\pm})} \times U(\mathrm{gd}(\mathrm{Im}(\vartheta^{\pm})) - \mathrm{Re}(\vartheta^{\pm}) - \phi) \quad (31a)$$

$$\zeta H_z^{\pm} = C_h^{\pm} e^{-jk_t\rho\cos(\phi+\vartheta^{\pm})} \times U(\mathrm{gd}(\mathrm{Im}(\vartheta^{\pm})) - \mathrm{Re}(\vartheta^{\pm}) - \phi) \quad (31b)$$

where $\mathrm{gd}(\cdot)$ denotes the Gudermann function. The corresponding expressions for the complex amplitudes of the surface waves are shown in (32) at the bottom of the next page. However, by resorting to the functional equations in (11) it comes out that (23), which guarantees the cancellation of the nonphysical poles for $n = 1/2$, also implies $C_e^{\pm} = C_h^{\pm} = 0$. Moreover, since both the spectral functions $s_e(\alpha)$ and $s_h(\alpha)$ are periodic with period $2\pi$ when $n = 1/2$, the diffracted field rigorously vanishes as well. As expected, for $n = 1/2$ this spectral solution reduces to the GO solution in agreement with the image principle.

## VI. Numerical Results

Samples of numerical results are provided in this section to numerically demonstrate that this solution smoothly reduces to all previous 3-D solutions for the right-angled impedance wedge problem with a perfectly conducting face. In all figures, we show the amplitude of the total field in the presence of a right-angled impedance wedge as a function of the observation angle $\phi$; the field is calculated at a constant distance ($k_t\rho = k\rho\sin\beta' = 10$) from the edge. The face $\phi = 0$ is characterized by a surface impedance tensor, while the other face ($\phi = 3\pi/2$) is perfectly conducting. A first example is reported in Fig. 3; the normalized impedance values along $z$ and $x$ are equal to $-4j$ and $0.25j$, respectively. Each curve plotted in the figure refers to a different value of the incidence skewness angle $\beta'$, while $\phi' = \pi/12$; the incident plane wave is TM$_z$ polarized ($E_z^i = 1, \zeta H_z^i = 0$). As apparent from Fig. 3(a), the amplitude of the copolar component of the total field ($E_z$) smoothly reduces to the continuous line, corresponding to the case of normal incidence, when the incidence skewness angle tends to $\pi/2$. The continuous line has been reported as a reference in the figure; it has been calculated by resorting to the rigorous Maliuzhinets solution [13], assuming an isotropic normalized surface impedance equal to $-4j$ on the loaded face ($\phi = 0$). As expected, the cross-polar component ($\zeta H_z$) of the total field continuously reduces at the increasing of $\beta'$, eventually vanishing for $\beta' = \pi/2$ (Fig. 3(b)). In order to give evidence to the scattering effects introduced by the anisotropic characteristics of the loaded face of the wedge, a further example is shown in Figs. 4(a) and (b). Again the incident wave is TM$_z$ polarized ($E_z^i = 1, \zeta H_z^i = 0$); its direction of incidence

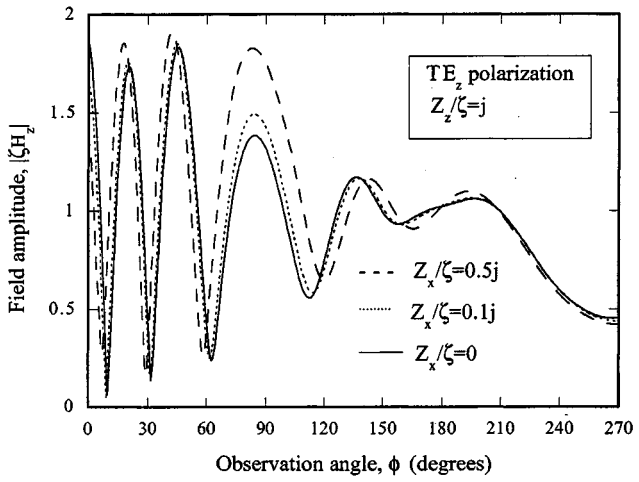


(a)

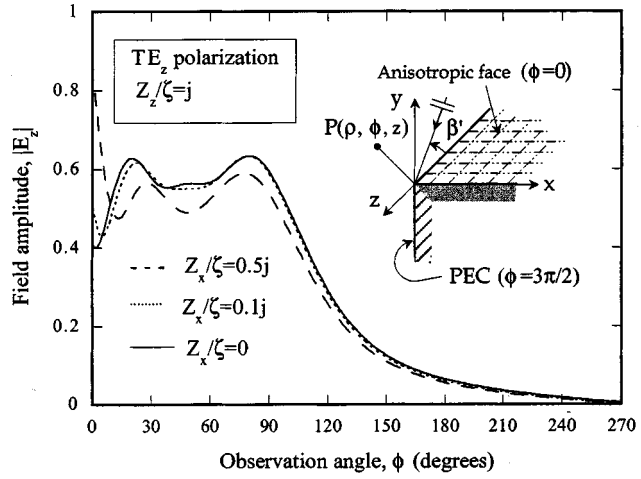


(b)

Fig. 7. Amplitude of the (a) co polar and (b) cross-polar longitudinal components of the total field in the presence of a right-angled impedance wedge with the face $\phi = 3\pi/2$ perfectly conducting. The wedge is illuminated by a TE$_z$ polarized ($E_z^i = 0, \zeta H_z^i = 1$) plane wave, impinging from $\beta' = \pi/4$, $\phi' = \pi/3$. The normalized surface impedance in the direction of the edge is $Z_z/\zeta = j$. Dashed lines: $Z_x/\zeta = 0.5j$; dotted lines: $Z_x/\zeta = 0.1j$; continuous lines: $Z_x/\zeta = 0$. The field is calculated at a normalized distance $k\rho \sin \beta' = 10$ from the edge.

is identified by the angles $\beta' = \pi/6$, $\phi' = \pi/12$. Four curves are plotted in both figures for different values of the tensor surface impedance on the loaded face ($\phi = 0$). In particular, the continuous line is related to a surface impedance tensor exhibiting the following normalized impedance values along the principal anisotropy axes: $Z_z/\zeta = -4j$, $Z_z/\zeta = 0.25j$. Conversely, the dashed-dotted line refers to a different surface impedance tensor with $Z_x/\zeta = -4j$, $Z_z/\zeta = 0.25j$. Finally, the dashed and the dotted lines refer to different isotropic impedance cases with normalized values $Z_z/\zeta = Z_x/\zeta = -4j$ and $Z_z/\zeta = Z_x/\zeta = 0.25j$, respectively.

A third example is reported in Fig. 5 to demonstrate that this solution smoothly converges to that for the isotropic impedance right-angled wedge [7], [8]. The incident plane wave impinges on the edge from $\beta' = \pi/4$, $\phi' = \pi/6$ and is TM$_z$ polarized ($E_z^i = 1, \zeta H_z^i = 0$). The surface impedance tensor on the loaded face ($\phi = 0$) is defined in terms of the parameter $\delta$: $Z_z/\zeta = -j(0.6 - \delta)$, $Z_x/\zeta = -j(0.6 + \delta)$. In particular, the dashed, dotted-dashed and dotted lines correspond to $\delta = 0.4$, $\delta = 0.2$, and $\delta = 0.02$, respectively. As is apparent, both the copolar [Fig. 5(a)] and the cross-polar [Fig. 5(b)] components of the field smoothly reduce to those obtained in the case of the corresponding isotropic impedance right-angled wedge ($\delta = 0$, continuous line) [7], [8].

In the remaining examples we check this solution against the rigorous ones determined for the right-angled wedge when the surface impedance in one of the principal anisotropy directions vanishes [9], [10]. In particular, the first case shown in Fig. 6(a) and (b) refers to a wedge with the loaded face ($\phi = 0$) exhibiting the following normalized surface impedance in the direction perpendicular to the edge: $Z_x/\zeta = 0.1 + 0.8j$, while the normalized surface impedance in the direction parallel to the edge assumes different values. The wedge is illuminated by a TE$_z$ polarized plane wave ($E_z^i = 0, \zeta H_z^i = 1$) impinging on the edge from $\beta' = \pi/4, \phi' = \pi/12$. In Fig. 6(a), the normalized surface impedance in the direction parallel to the edge is equal to: $Z_z/\zeta = j$ (dashed line), $Z_z/\zeta = 0.2j$ (dotted line) and $Z_z/\zeta = 0$ (continuous line). The continuous line in Fig. 6(a) has been plotted as a reference; it has been evaluated by resorting to the asymptotic approximation of the rigorous solution proposed in [10]. We observe that the amplitude of the copolar component of the field plotted in Fig. 6(a) tends to the continuous line when the value of $Z_z/\zeta$ decreases, eventually overlapping with the continuous line in the limit $Z_z/\zeta = 0$. In Fig. 6(b), the normalized surface impedance in the direction parallel to the edge is equal to: $Z_z/\zeta = j$ (dashed line), $Z_z/\zeta = 0.5j$ (dashed-dotted line), $Z_z/\zeta = 0.2j$ (dotted line) and $Z_z/\zeta = 0.1j$ (continuous line). As apparent, the amplitude of the cross-polar component in Fig. 6(b) decreases when the modulus of $Z_z/\zeta$ decreases; it exactly vanishes for $Z_z/\zeta = 0$, as expected. In fact, in the latter case the IBC's on the loaded face decouple [see (5)] so that a cross-polar component is not present anymore. A last example

$$C_e^{\pm} = \frac{-\left(\sin\vartheta^{\pm} - \sin\beta' \frac{Z_x}{\zeta}\right) t_{\mathcal{E}}\left(-\pi - \vartheta^{\pm} - \frac{n\pi}{2}\right) + \cos\beta' \cos\vartheta^{\pm} t_{\mathcal{H}}\left(-\pi - \vartheta^{\pm} - \frac{n\pi}{2}\right)}{\pm \sin\beta' \cos\vartheta^{\pm}(\sin\vartheta^{+} - \sin\vartheta^{-})} \tag{32a}$$

$$C_h^{\pm} = \frac{-\left(\sin\vartheta^{\pm} - \sin\beta' \frac{\zeta}{Z_z}\right) t_{\mathcal{H}}\left(-\pi - \vartheta^{\pm} - \frac{n\pi}{2}\right) - \cos\beta' \cos\vartheta^{\pm} t_{\mathcal{E}}\left(-\pi - \vartheta^{\pm} - \frac{n\pi}{2}\right)}{\pm \sin\beta' \cos\vartheta^{\pm}(\sin\vartheta^{+} - \sin\vartheta^{-})}. \tag{32b}$$

is shown in Figs. 7(a) and (b). Again the incident plane wave is $TE_z$ polarized ($E_z^i = 0, \zeta H_z^i = 1$); it impinges from a direction determined by the angles $\beta' = \pi/4, \phi' = \pi/3$. This time we fix the value of the normalized impedance in the direction parallel to the edge: $Z_z/\zeta = j$. Conversely, the normalized surface impedance along $x$ varies as follows: $Z_x/\zeta = 0.5j$ (dashed line), $Z_x/\zeta = 0.1j$ (dotted line), $Z_x/\zeta = 0$ (continuous line). Again, the continuous line has been plotted in both Figs. 7(a) and (b) as a reference; it has been calculated by resorting to the uniform asymptotic evaluation of the rigorous solution in [9]. It is seen that when the modulus of $Z_x/\zeta$ decreases this solution converges to that in [9], both for the co-polar (Fig. 7(a)) and the cross-polar (Fig. 7(b)) components of the total field.

We finally note that, as apparent in all plots reported in this section, the solution proposed is uniform also at the shadow boundaries of the surface waves excited by the diffraction phenomenon at the edge and propagating along the loaded face of the wedge.

## VII. Conclusion

A rigorous spectral solution for the scattering by a right-angled anisotropic impedance wedge with a perfectly conducting face has been presented, when the wedge is illuminated by an arbitrarily polarized plane wave impinging at oblique incidence on its edge. The surface impedance tensor on the loaded face of the wedge may exhibit arbitrary values, but the principal anisotropy directions must be parallel and perpendicular to the edge of the wedge. The solution is determined by resorting to the Sommerfeld–Maliuzhinets method and is expressed in a simple closed form, containing only ratios of trigonometric functions. It recovers as limit cases all previous 3-D solutions for the right-angled impedance wedge with a perfectly conducting face. Uniform asymptotic expressions have been derived from the above spectral solution in the framework of UTD; they provide a continuous behavior of the fields also at the shadow boundary of the surface waves, which can be excited by the diffraction phenomenon at the edge and propagate along the loaded face of the wedge.

## References


[1] T. B. A. Senior and J. L. Volakis, *Approximate Boundary Conditions in Electromagnetics—IEE Electromagn. Wave Ser.*. London, U.K.: Inst. Elect. Eng., 1995, vol. 41.

[2] S. A. Tretyakov, "On the homogenization of dense planar arrays of scatterers," *Electromagn.*, vol. 19, pp. 201–210, 1999.

[3] N. Marcuvitz, *Waveguide Handbook*, 2nd ed. London, U.K.: Inst. Elect. Eng., Peter Peregrinus, 1995, p. 280. *et seq*.

[4] N. V. Shuley and R. J. Langley, "Method for treatment of finite-sized dichroic structures using a surface impedance approach," *Electron. Lett.*, vol. 24, no. 12, pp. 728–729, 1988.

[5] K. W. Whites and R. Mittra, "An equivalent boundary-condition model for lossy planar periodic structures at low frequencies," *IEEE Trans. Antennas Propagat.*, vol. 44, pp. 1617–1628, Dec. 1996.

[6] G. Manara, P. Nepa, and G. Pelosi, "EM scattering from anisotropic impedance wedges at oblique incidence—Application to artificially hard and soft surfaces," *Special Issue Centennial Sommerfeld's Diffraction Problem—Electromagn.*, vol. 18, no. 2, pp. 117–133, 1998.

[7] R. G. Rojas, "Electromagnetic diffraction of an obliquely incident plane wave field by a wedge with impedance faces," *IEEE Trans. Antennas Propagat.*, vol. 36, pp. 956–970, July 1988.

[8] V. G. Vaccaro, "Electromagnetic diffraction from a right-angled wedge with soft conditions on one face," *Opt. Acta*, vol. 28, no. 3, pp. 293–311, 1981.

[9] G. Manara, P. Nepa, and G. Pelosi, "Electromagnetic scattering by a right angled anisotropic impedance wedge," *Electron. Lett.*, vol. 32, no. 13, pp. 1179–1180, 1996.

[10] ——, "A UTD solution for plane wave diffraction at an edge in an artificially hard surface: Oblique incidence case," *Electron. Lett.*, vol. 31, no. 19, pp. 1649–1650, 1995.

[11] P.-S. Kildal, "Artificially hard and soft surfaces in electromagnetics," *IEEE Trans. Antennas Propagat.*, vol. 38, pp. 1537–1544, Oct. 1990.

[12] G. Manara and P. Nepa, "Electromagnetic scattering from a right-angled anisotropic impedance wedge with a perfectly conducting face," in *Nat. Radio Sci. Meet.*, Boulder, CO, Jan. 1998, p. 237.

[13] G. D. Maliuzhinets, "Excitation, reflection and emission of surface waves from a wedge with given face impedances," *Sov. Phys. Dokl.*, no. 3, pp. 752–755, 1958.

[14] ——, "Inversion formula for the Sommerfeld integral," *Sov. Phys. Dokl.*, no. 3, pp. 52–56, 1958.

[15] R. G. Kouyoumjian, G. Manara, P. Nepa, and B. J. E. Taute, "The diffraction of an inhomogeneous plane wave by a wedge," *Radio Sci.*, vol. 31, no. 6, pp. 1387–1397, Nov./Dec. 1996.

[16] R. G. Kouyoumjian and P. H. Pathak, "A uniform geometrical theory of diffraction for an edge in a perfectly conducting surface,," *Proc. IEEE*, vol. 62, pp. 1448–1461, Nov. 1974.

[17] G. Manara, P. Nepa, R. G. Kouyoumjian, and B. J. E. Taute, "The diffraction of an inhomogeneous plane wave by an impedance wedge in a lossy medium," *IEEE Trans. Antennas Propagat.*, vol. 46, pp. 1753–1755, Nov. 1998.



**Giuliano Manara** (M'88–SM'93) was born in Florence, Italy, on October 30, 1954. He received the Laurea (Doctor) degree in electronics engineering (*summa cum laude*) from the University of Florence, Italy, in 1979.

He was first with the Department of Electronics Engineering, University of Florence as a Postdoctoral Research Fellow. In 1987 he joined the Department of Information Engineering, University of Pisa, Italy, where he currently works as a Full Professor. Since 1980 he has been collaborating with the Department of Electrical Engineering, The Ohio State University, Columbus, OH, where, in the summer and fall of 1987, he was involved in research at the ElectroScience Laboratory. His current research interests include numerical and asymptotic techniques as applied to electromagnetic scattering and radiation problems (both in frequency and time domain), scattering from rough surfaces, and electromagnetic compatibility.



**Paolo Nepa** (M'95) was born in Teramo, Italy, on August 7, 1965. He received the Laurea (Doctors) degree in electronics engineering (*summa cum laude*) from the University of Pisa, Italy, in 1990.

After 1990, he joined the Department of Information Engineering of the same university where he is presently an Assistant Professor. In 1998, supported by a grant from the Italian National Research Council, he was a Visiting Scholar at the ElectroScience Laboratory, The Ohio State University, Columbus, OH, where he was involved in research on efficient hybrid techniques for the analysis of large antenna arrays. His current research interests also include the development and application of uniform asymptotic techniques in electromagnetic scattering.

Dr. Nepa received the "Young Scientist Award" from the International Union of Radio Science Commission B in 1998.